Urol Res (2000) 28:404–415

ORIGINAL PAPER

A. Schmiedl · P. O. Schwille · E. Bonucci
R. G. Erben · A. Grayczyk · V. Sharma

Nephrocalcinosis and hyperlipidemia in rats fed a cholesterol- and fat-rich diet: association with hyperoxaluria, altered kidney and bone minerals, and renal tissue phospholipid–calcium interaction

Received: 12 April 2000 / Accepted: 3 August 2000

Abstract To determine whether an "atherogenic" diet (excess of cholesterol and neutral fat) induces pathological calcification in various organs, including the kidney, and abnormal oxalate metabolism, 24 male Sprague-Dawley rats were fed either normal lab chow (controls, $n = 12$) or the cholesterol- and fat-rich experimental diet (CH-F, $n = 12$) for 111 ± 3 days. CH-F rats developed dyslipidemia [high blood levels of triglycerides, total, low-density lipoprotein (LDL)-, very low-density lipoprotein (VLDL)-, high-density lipoprotein (HDL)-bound cholesterol, total phospholipids], elevated serum total alkaline phosphatase and lactate dehydrogenase (LDH) levels, in the absence of changes in overall renal function, extracellular mineral homeostasis [serum protein-corrected total calcium, magnesium, parathyroid hormone (PTH), 1,25-dihydroxyvitamin D ($1,25(OH)_2D$)], plasma glycolate and oxalate levels. There was a redistribution of bone calcium and enhanced exchange of this within the extraosseous space, which was accompanied by significant bone calcium loss, but normal bone histomorphometry. Liver oxalate levels, if expressed per unit of defatted (DF) dry liver, were three times higher than in the controls. Urinary glycolate, oxalate, calcium and total protein excretion levels were elevated, the latter showing an excess of proteins > 100 kD and a deficit of proteins > 30–50 kD. Urinary calcium oxalate supersaturation was increased, and calcium phosphate supersaturation was unchanged. There were dramatically increased (by number, circumference, and area) renal calcium phosphate calcifications in the cortico-medullary region, but calcium oxalate deposits were not detectable. Electron microscopy (EM) and elemental analysis revealed intratubular calcium phosphate, apparently needle-like hydroxyapatite. Immunohistochemistry of renal tissue calcifications revealed co-localization of phospholipids and calcium phosphate. It is concluded that rats fed the CH-F diet exhibited: (1) a spectrum of metabolic abnormalities, the more prominent being dyslipidemia, hyperoxaluria, hypercalciuria, dysproteinuria, loss of bone calcium, and calcium phosphate nephrocalcinosis (NC); and (2) an interaction between calcium phosphate and phospholipids at the kidney level. The biological significance of these findings for the etiology of idiopathic calcium urolithiasis in humans is uncertain, but the presented animal model may be helpful when designing clinical studies.

Key words Cholesterol-rich diet · Hyperlipidemia · Nephrocalcinosis · Phospholipid–calcium interaction · Calcium phosphate deposits · Hyperglycoluria and hyperoxaluria

Supported by the W. Sander Foundation for the Advancement of Medical Sciences, Munich, Germany

Parts of this work were published in the Proceedings of 8th European Symposium on Urolithiasis, 9–12 June 1999, Parma, Italy

A. Schmiedl (✉)
c/o Paul O. Schwille,
University Hospital – Department of Surgery,
Maximiliansplatz 2, 91023 Erlangen, Germany

A. Schmiedl · P. O. Schwille · A. Grayczyk · V. Sharma[1]
Mineral Metabolism and Endocrine Research Laboratory,
Departments of Surgery and Urology,
University of Erlangen, Germany

E. Bonucci
Department of Experimental Pathology,
University of Rome, Italy

R. G. Erben
Institute of Animal Physiology,
Ludwig-Maximilian University, Munich, Germany

Permanent Address:
[1]College of Agricultural Sciences, Jobner, India

Introduction

Nephrocalcinosis (NC) in humans, especially when it occurs in the cortico-medullary and papillary regions, is considered to be an early event in renal calcium stone formation [13, 18, 42, 60]. Recently, disordered lipids, in particular cholesterol excess, have increasingly been

attracting the interest of investigators as possible factors underlying NC and its role in the development of urinary tract stones. For example, the simultaneous occurrence of hypercholesterolemia and renal stones has been used as an indicator of death rates in the general population [63–65]; dyslipidemia, including hypercholesterolemia, has been demonstrated in patients with idiopathic calcium urolithiasis [48, 52, 62]; lipids are contained in both the mineral portion and the proteinaceous matrix of calcium-containing urinary tract stones [26]; and urinary hyperexcretion of lipids has been observed in patients forming renal calcium stones [25]. Thus, a close relationship may exist between pathological renal calcifications and lipids. In humans, however, ethical and technical considerations prohibit more in-depth investigations into the role of nutrition and the resulting sequence of events at the renal tissue level. In the rat, in contrast, renal cortico-medullary NC develops in response to such dietary challenges as magnesium deficit [10, 49], excess of protein and phosphorus [70], and excess of cholesterol [51]; NC may be accompanied by calcium phosphate stones in the pyelo-calieceal region [51].

Stones formed by humans consist of calcium oxalate and, when analyzed using sensitive techniques, are found to contain calcium phosphate, which is mainly located in the core [30]. A realistic speculation is, therefore, that calcium phosphate NC plays a role during the early periods of the stone-forming processes, and that the formation of stones containing an excess of calcium oxalate over calcium phosphate necessitates periods of hyperoxaluria, hypercalciuria, or both, resulting in elevated supersaturation of urine with stone salts. Lipid- and fatty acid-related hyperoxaluria and hypercalciuria have been observed [28, 29, 57]. Irrespective of the degree of calciuria, osteopenia is frequent in patients with idiopathic renal calcium stones [5, 47] and in those with atherosclerosis due to disordered lipids [28]. This suggests that the calcium content of kidneys, bones and arteries is in some way dictated by lipid–calcium interactions. Thus, an animal model of dyslipidemia exhibiting not only calcium phosphate NC, but also abnormalities of oxalate, extracellular and tissue minerals, and tissue morphology, would be desirable. Therefore, the aim of the present work was to test whether long-term exposure to a dietary excess of cholesterol and lipids (so-called ''atherogenic'' diet) results into such abnormalities. If the answer is yes, their co-existence would be helpful for understanding the etiology of idiopathic renal calcium stones.

We report on the nature and quantity of kidney calcifications, liver, kidney and urinary oxalate, bone, extraosseous, especially kidney, minerals, and bone histology, in rats fed an ''atherogenic'' diet. The main perception gained was that long-term exposure of rats to excess dietary cholesterol and fat does not lead to urinary tract stones that are visible to the naked eye. However, the renal medulla is predisposed to the deposition of calcium phosphate, not calcium oxalate, which results in urinary hyperexcretion of glycolate and oxalate, and impairs bone calcium despite unchanged serum calcium, parathyroid hormone (PTH) and 1,25-dihydroxyvitamin D ($1,25(OH)_2D$) levels.

Materials and methods

Animals

All investigations were approved by the Ethics Committee as required by the German Law Against Cruelty to Animals. Twenty-four male Sprague-Dawley rats (Wiga, Sulzfeld, Germany), weighing approximately 200 g each, were housed in individual cages under a 12-h light and 12-h dark cycle. The rats were acclimatized for 1 week prior to experimentation, during which time they had free access to tap water and normal rat chow.

Experimental design

During the experimental period, animals received demineralized water ad libitum, and were randomly assigned to one of two groups:

- Pelleted normal diet (control; $n = 12$), containing (per kg dry matter) 50.83 g crude fat, but no cholesterol (C 1000; Altromin, Lage, Germany);
- Pelleted cholesterol- and fat-rich diet (CH-F; $n = 12$), containing (per kg dry matter) 10.0 g cholesterol, 20.0 g sodium-cholate, and 112.0 g crude fat (C 1061, modified; Altromin, Lage, Germany).

The mineral and oxalate content (g/kg dry matter) of the two diets was as follows (control/CH-F): calcium 9.5/9.3; magnesium 0.74/0.73; total phosphorus 7.5/7.3; oxalate 0.6/0.7 (own analysis); glycolate and phospholipids were not present. Compared with the normal diet (control), the ''atherogenic'' diet (CH-F) contains less mono- and polyunsaturated fatty acids (synonym: essential fatty acids), especially oleic and linoleic acid, and is devoid of eicosaenic and eicosadienic acid, which are precursors of the arachidonic acid–prostaglandin cycle. The available energy/kg dry matter was 3097 (control) and 3585 (CH-F) kcal. The duration of the experiment was 111 ± 3 days.

The excess of cholesterol and neutral fat in the CH-F diet was selected to approximate the ''high-fat food'' generally eaten in numerous westernized populations. Preliminary experiments with the CH-F diet revealed that urinary malonedialdehyde, which is indicative of lipid peroxidation [11], was not increased (control 859 and CH-F 509 nmol/mmol creatinine), and that serum beta-carotene, which is indicative of intestinal malabsorption [31], was not decreased (control 34 and CH-F 46 mg/dl). This is in contrast to a diet containing less cholesterol that stimulated oxidative metabolism [12], which itself constitutes a risk factor for atherosclerosis [59].

Procedures and collection of samples

Water and the respective diet were offered throughout the experiment. Prior to termination of the experiments, all animals were labeled with ^{45}calcium, as described elsewhere [66], to allow assessment of the intrabone distribution of calcium and its exchange with the intravascular space. Urine was collected under paraffin while rats were housed in metabolism cages. For analysis of oxalate and glycolate, aliquots of urine were stored at −80 °C. From fasting (18 h) and anesthetized [intraperitoneally (IP) administered sodium pentobarbital (Nembutal, Abbott, Lage, Germany) at 45 mg/kg body weight] rats, we determined the blood gases and hematocrit (in arteriovenous blood from the incised tail); thereafter, the animals were exsanguinated by bleeding from the abdominal aorta. Plasma and serum were stored at −20 °C. The

abdominal aorta was removed from a few animals, and the liver, right femur, right tibia, first lumbar vertebra, and kidneys were removed from the majority of animals. The right kidney was cut longitudinally and processed for light and electron microscopy (EM) (see below). The left kidney was decapsulated, cut longitudinally, and specimens were taken from the cortical and medullary (approx. 100 mg), and the papillary (approx. 30 mg) regions. The remaining tissue was shock-frozen in liquid nitrogen, and stored at −80 °C. Prior to analysis, tissues were dried at 100 °C overnight; ash from the incinerated kidney and aorta (at 450 °C, 12 h) and from the femur (at 800 °C, 24 h) was weighed and dissolved in 6 M hydrochloric acid (HCl). Aliquots from undefatted (unDF) liver were extracted in 0.1 M HCl; other DF aliquots were extracted in ethanol/chloroform (1/3; v/v), and, following lyophilization, the dry weight was assessed.

Histology

The right half of the kidneys of six of the rats was fixed in 4% buffered formalin and embedded in paraffin; 5-μm thick slices were obtained from each paraffin block and mounted. Initial examinations of kidney sections from rats fed the atherogenic diet were negative for calcium oxalate when stained using the specific method of Yasue [67]. To detect calcium-containing deposits, slices were stained using the method of Gallyas and Wolff [19], which is unable to differentiate between calcium phosphate and calcium oxalate. The areas of the deposits were identified by light microscopy and quantified by computerized image analysis, using the appropriate software (Global Lab, Data Translation, Bietigheim-Bissingen, Germany) and hardware (CCD-Camera B/W BC-1, AVT-Horn, Aalen, Germany). The number of deposits, their area and their circumference were assessed in a segment obtained from one of the kidney halves of each of the six animals; this segment was the middle of the three theoretical 60° segments obtained, taking the greatest horizontal diameter of the kidney as the geometrical basis. Because all kidneys were of a similar size, the area of this segment varied only minimally. For EM, cubes of approx. 1 mm^3 were cut from a calcified slice of a CH-F rat, fixed with 2.5% glutaraldehyde/formalin, post-fixed with 1% osmium tetroxide, and embedded in epoxy resin. Ultrathin sections were contrasted with uranyl acetate and lead citrate, and examined at 80 keV by scanning transmission electron microscopy (TEM; Philips CM 200, Philips, Eindhoven, The Netherlands). Energy dispersive X-ray analysis (EDX, EDAX DX-4; EDAX, Mahwah, N.J., USA) of electron-dense areas, and element mapping of quadrants of single renal tubular cells were performed to detect changes in the intracellular distribution of calcium, magnesium, and phosphorus.

From one control and one CH-F rat, the other half of the right kidney was examined for lipid deposition-associated calcifications. Six slices were obtained and mounted: five slices were decalcified and stained for neutral lipids with Sudan black B and Oil red, and for cholesterol using the method of Schultz, as modified by Lewis and Lobban [32]. The remaining slices were reacted immunohistochemically with the antibody MC22 33F to detect choline-containing phospholipids, as described by Bonucci et al. [8].

The tibia and the first lumbar vertebra were examined by light microscopy using previously described procedures [44, 45].

Clinical chemistry and other methods

Both routine and more sensitive analytical methods were used. The former included: blood gases and urinary total CO_2 (pH/Blood Gas Analyzer 1306, Instrumentation Laboratory, Milan, Italy); urinary pH (glass electrode); creatinine (colorimetry) and glucose (Gluco-Analyzer, Beckman, Fullerton, Calif., USA) in serum and urine; total protein in serum (refractometry) and urine (colorimetry; chemicals from Bio-Rad Laboratories, Munich, Germany); serum total alkaline phosphatase (colorimetry; kit from Merck, Darmstadt, Germany); total cholesterol and high-density lipoprotein (HDL)-bound cholesterol; triglycerides; free fatty acids; lactate dehydrogenase (DLH) (all kits from Boehringer, Mannheim, Germany); phospholipids (kit from bioMérieux, Nürtingen, Germany); in tissue ash; serum and urine calcium and magnesium (flame atomic absorption spectrometry; Elektrolyt-Automat FL 6, Zeiss, Oberkochen, Germany); and phosphorus (colorimetry). Among the more specialized determinations were: glycolate and oxalate in HCl tissue extract, plasma and urine [35]; urinary malonedialdehyde [11], citrate, and bone collagen crosslinks in urine [all by high performance liquid chromatography (HPLC; Dionex 2000i, Dionex, Sunnyvale, Calif., USA)]; urinary ammonia (Berthelot's reaction); serum bone isoenzyme of alkaline phosphatase (electrophoresis and densitometry; reagents: Isopal-Paragon, Beckman); PTH; $1,25(OH)_2D$ (radioimmunoassay kits from Nichols, Bad Nauheim, Germany); and beta-carotene (colorimetry) [31]; in serum and bone ash, ^{45}calcium was counted, and subsequently corrected for decay. Determination of the bone-breaking force has been described elsewhere [66]. Protein in native and sieve-fractionated (see below) urine was measured by the Lowry method; because the amounts of urine of control and CH-H rats were limited, aliquots from several rats were pooled to obtain one sufficiently large sample per group. This was vacuum-suctioned through filters (Millipore, Eschborn, Germany) with pore sizes that enabled the retention of proteinaceous particles >100, >50, >30, and >10 kD. Bone volume and the mean specific density were determined by Archimedes' principle.

Calculations and statistics

Serum low-density lipoprotein (LDL)-bound cholesterol and very low-density lipoprotein (VLDL)-bound cholesterol were calculated using the standard formula [6] and the ratio triglycerides/5, respectively. Relative supersaturation products (RSP) in urine were computed from solubility products [36]. Bone minerals were expressed per unit volume of bone. The exchangeable bone calcium fraction was taken as the ratio of ^{45}calcium-specific activity in serum and bone. The number of calcified patches of each kidney sector selected were counted, and the median area of patches, the total area, the median circumference, and the sum of circumferences were assessed. Results in serum and urine (average of two collection days) were given as mean values (SEM, or range). Between-group differences were tested for significance ($P \leq 0.05$) by the *t*- or the *U*-test, as appropriate.

Results

Tolerance of the CH-F diet, course of body weight, findings at autopsy, and blood lipids

The experimental diet was well tolerated, but the rats showed less (between 4 and 10%) body weight gain during the 17-week observation period (Fig. 1), resulting in a lower final body weight than the controls (Table 1). Food and fluid intake, as well as hematocrit, were unsuspicious (Table 1), as were blood gases (not shown), but fecal color and consistency changed to light and greasy, respectively. The livers of CH-F rats appeared to be enlarged with blunt edges, and were yellowish and pale. The gross anatomy of the kidneys and other organs was unremarkable (for kidney histology, see the "Renal calcifications, TEM and EDX, lipid deposition and immunohistochemistry" section), and the urinary tract was stone-free. Serum levels of total, HDL-, LDL-, VLDL-bound cholesterol, triglycerides and total phospholipids were elevated, and, owing to the proportionally greater LDL increase, the HDL/LDL ratio was decreased; free fatty acids were unchanged. Glycemia and urinary

glucose excretion were comparable in the two groups (data not shown).

Extracellular minerals and other substances, tissue oxalate and minerals

Serum or plasma (Table 2)

Serum total protein was elevated, and there was a 2.5-fold increase in LDH; other parameters, such as protein-corrected calcium, ^{45}calcium-specific activity, PTH, $1,25(OH)_2D$, glycolate and oxalate were within the ranges seen in the controls.

Urine (Table 2)

There was a significant increase in urinary volume, pH, CO_2, sodium, calcium, total protein, ammonium and citrate, as also in glycolate, oxalate, and the RSP of calcium oxalate; phosphorus was slightly decreased; other changes were borderline or insignificant.

Filtration of urine through membranes with decreasing molecular cut-off (see "Material and methods" section) yielded the following data (given as percentage of total protein concentration of respective filtrate): control diet 45, 4, 41, 2, and 7; CH-F diet 89, 3, 2, 0.1, and 6. Accordingly, proteins of >100 and >30–50 kD appear to be predominant in the urine of rats fed a normal diet, while there appears to be a deviation from the normal protein spectrum (large excess of >100 kD and a deficit in >30–50 kD proteins) in the urine of rats fed the NC-inducing CH-F diet. It is worth noting that proteins of approx. 30 kD are under discussion as inhibitors of the crystallization of stone-forming salts [3, 23, 58]. Unfortunately, the microscopic evaluation of urinary crystals was unreliable due to artifacts caused by the presence of non-crystallized particulate matter.

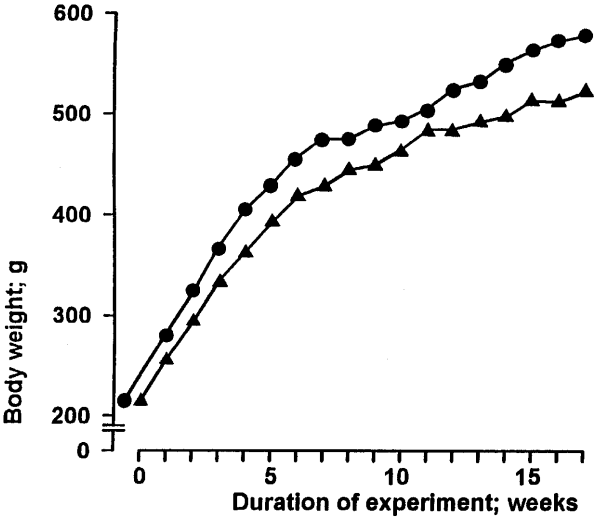

Fig. 1 Course of mean body weight of rats fed a normal (●) or CH-F (▲) diet. For further information, see Table 1 and text

Tissue glycolate, oxalate and citrate (Table 2)

Liver glycolate and oxalate, expressed per unit dry weight of unDF tissue, were not elevated in CH-F rats. Because DF liver weighed approx. 25% (control) and 75% (CH-F) less than unDF liver, the presented low mean oxalate content per unit unDF liver of CH-F rats may be misleading. Extrapolation of oxalate on the basis of DF liver dry weight would yield mean values of 579 (control) and 1564 (CH-F) nmol/g, respectively; the latter value is compatible with oxalate overproduction. Kidney oxalate and citrate content was statistically unchanged.

Renal tissue minerals (Fig. 2)

In control rats, the well known cortico-medullary-papillary step-up gradient of minerals occurred, especially for calcium and magnesium. The CH-F diet evoked significant increases in cortical calcium and medullary phosphorus, and an increase of magnesium in all three anatomical regions, meaning a higher ratio of calcium/phosphorus and calcium/magnesium.

Table 1 Initial and final body weight, and lipids at the end of experiments as found in the fasting plasma of rats fed the normal diet (control) or the cholesterol-rich diet (CH-F) over the study period. Values are expressed as the mean, with the standard error given in parentheses. *LDL* low-density lipoprotein, *VLDL* very low-density lipoprotein, *HDL* high-density lipoprotein

	Control $n = 12$		CH-F $n = 12$		*P*-value
Initial body weight (g)	213	(3)	216	(2)	0.45
Final body weight (g)	580	(18)	525	(10)	0.02
Food intake (g/day)	10.5	(0.9)	14.0	(2.1)	0.14
Fluid intake (ml/day)	17	(2)	21	(3)	0.22
Hematocrit (%)	47	(1)	46	(1)	0.17
Triglycerides (mg/dl)	21	(3)	38	(4)	0.002
Total cholesterol (mg/dl)	51	(4)	334	(36)	<0.001
HDL cholesterol (mg/dl)	28	(2)	54	(6)	<0.001
Total cholesterol/HDL	1.9	(0.2)	7.0	(1.2)	<0.001
LDL cholesterol (mg/dl)	20	(4)	272	(36)	<0.001
HDL/LDL	1.9	(0.3)	0.23	(0.04)	<0.001
VLDL cholesterol (mg/dl)	4.2	(0.5)	7.6	(0.9)	0.002
Total phospholipids (g/l)	0.68	(0.04)	1.16	(0.07)	<0.001
Free fatty acids (mM/l)	0.89	(0.03)	0.85	(0.04)	0.44

Table 2 Variables in serum or plasma, and urine, of relevance for the state of extracellular mineral homeostasis, oxalate, and proteins. For further details, see "Material and methods" section. Values are expressed as the mean, with the SE given in parentheses. *Cr* urinary creatinine, *SA* specific activity, *LDH* lactate dehydrogenase; *1,25(OH)$_2$D* 1,25-dihydroxyvitamin D, *RSP* relative supersaturation products

	Control $n = 12$[a]		CH-F $n = 12$[a]		*P*-value
Plasma					
Creatinine (mg/dl)	0.71	0.03)	0.73	(0.03)	0.71
Total protein (g/dl)	5.5	(0.1)	6.4	(0.2)	< 0.001
Total calcium corrected[d] (mg/dl)	11.3	(0.1)	11.1	(0.2)	0.31
Total calcium (mg/dl)	10.0	(0.1)	10.3	(0.1)	0.06
Magnesium (mg/dl)	1.8	(0.1)	1.9	(0.1)	0.30
Phosphorus (mg/dl)	5.4	(0.3)	4.9	(0.2)	0.22
PTH (pg/ml)	73	(16)	42	(6)	0.08
1,25$(OH)_2$D (pg/ml)	14	(1)	16	(1)	0.33
Total alkaline phosphatase (IU/l)	78	(8)	259	(23)	< 0.001
LDH (IU/l)	137	(12)	350	(38)	< 0.0001
Glycolate (μmol/l)	8.4	(0.3)	8.6	(0.6)	0.75
Oxalate (μmol/l)	3.9	(0.5)	4.6	(0.5)	0.29
^{45}Calcium-SA [(cpm/μmol) × 10^{-3}]	0.34	(0.01)	0.33	(0.02)	0.61
Tissue					
Liver glycolate (nmol/g)[b]	480	(43) [5]	391	(24) [5]	0.11
Liver oxalate (nmol/g)[b]	434	(33) [9]	391	(28) [10]	0.34
Kidney oxalate (nmol/g)[b]	7.2	(1.4) [7]	5.3	(0.7) [11]	0.21
Kidney citrate (nmol/g)[b]	602	(154) [6]	1974	(580) [10]	0.10
Urine					
Volume (ml)[c]	6.8	(0.5)	10.4	(1.3)	0.02
pH	6.4	(0.1)	6.9	(0.2)	0.009
Total CO_2 (mmol/l)	1.3	(0.1)	3.9	(1.0)	0.02
Ammonium/Cr (mmol/mmol)	5.54	(0.34) [11]	3.62	(0.37) [11]	0.001
Citrate/Cr (μmol/mmol)	536	(53)	1368	(163)	< 0.001
Calcium/Cr (μmol/mmol)	115	(18)	166	(16)	0.05
Magnesium/Cr (μmol/mmol)	458	(30)	468	(48)	0.87
Phosphorus/Cr (mmol/mmol)	10.5	(0.8)	8.5	(0.6)	0.04
Glycolate/Cr (μmol/mmol)	39	(4)	62	(4)	< 0.001
Oxalate/Cr (μmol/mmol)	34	(6)	68	(4)	< 0.001
Potassium/Cr (mmol/mmol)	13	(1)	17	(2)	0.07
Sodium/Cr (mmol/mmol)	26	(2.9)	35	(3.3)	0.05
RSP calcium oxalate	1.17	(0.03)	1.29	(0.04)	0.03
RSP brushite	1.12	(0.06)	1.25	(0.11)	0.30
Total protein/Cr (μg/mmol)	2.1	(0.5) [10]	20	(5.5)	0.0002*
Albumin/Cr (μg/mmol)	0.016	(0.004) [8]	0.056	(0.025)	0.15*

* Based on $\log_{10}$ of values
[a] Except for values in square brackets [ ]
[b] Dry weight
[c] Per day
[d] For mean serum total protein of control

Renal calcifications, TEM and EDX, lipid deposition and immunohistochemistry

Calcifications

An overview of the CH-F diet-induced cortico-medullary calcification (synonymous with NC) and a detailed description of its morphology have previously been published [46, 51, 54]. Briefly, the major histological characteristics of this type of NC were as follows: the organs were free of clusters of lymphocytes, granulocytes or macrophages, signifying that no light-microscopically detectable interstitial inflammation developed; calcium-positive deposits were found inside the tubular lumina of the cortico-medullary border and the outer medulla, but the cortex and papilla were calcification-free; and the calcifications were ovoid or circular, in the latter case being organized as several layers around a central core. With increasing size, the calcifications became irregularly shaped, frequently filling and dilating the tubular lumen. Often, the adjacent tubular epithelium appeared flat or eroded in such a way that the epithelium could not be identified as belonging to the descending or the ascending part of the loop of Henle; occasionally, cellular membranes seemed to adhere to the surface of calcifications.

Table 3 shows the quantitative data of calcifications. In each kidney of the six CH-F rats, the calcification-covered tissue area was enormous, while calcifications were present in only two of six control kidneys. Large calcifications were characteristic for CH-F rats, manifesting as an increase in total circumference and total area (approx. 7.5- and 7-fold, respectively); smaller solitary concretions in both groups were comparable in terms of circumference and area.

TEM and EDX

TEM also revealed that the concretions appeared to have a central core and an outer zone, both regions presenting as an accumulation of compact electron-dense bodies, in general inwardly less abundant (Fig. 3a). Whether these bodies represent "lipids" or calcium phosphate deposits could not be determined. Similarly, electron-dense material was found intraluminally in close vicinity to the membranes of cells lining the tubular lumen; it was surrounded by a needle-like

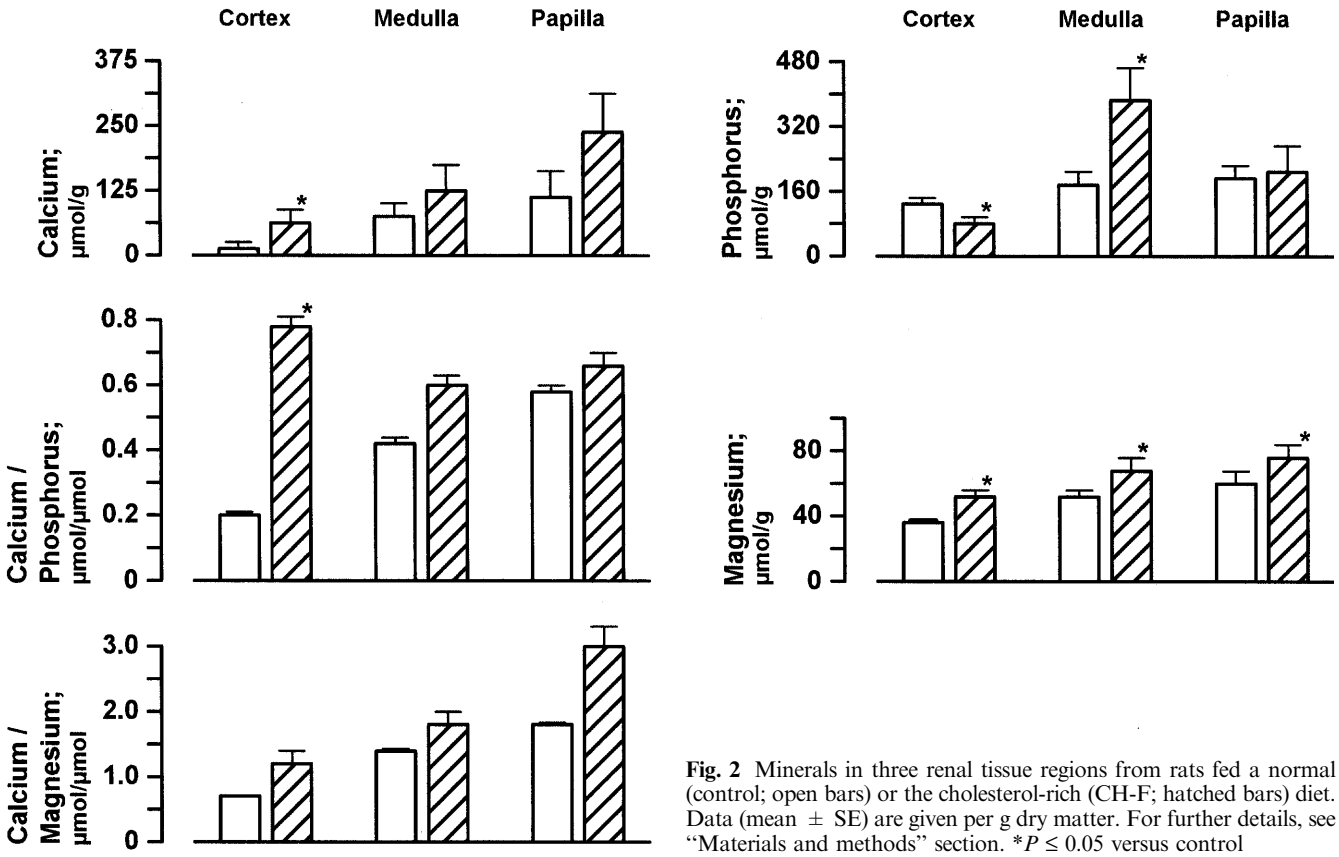

Fig. 2 Minerals in three renal tissue regions from rats fed a normal (control; open bars) or the cholesterol-rich (CH-F; hatched bars) diet. Data (mean ± SE) are given per g dry matter. For further details, see "Materials and methods" section. *$P \leq 0.05$ versus control

Table 3 Renal calcifications as quantified by number, circumference, and area. Σ, sum of individual values. Values are expressed as the mean (minimum; maximum). For technical and other details, see "Materials and methods" and "Results" sections

	Control $n = 6$		CH-F $n = 6$		*P*-value
Calcifications (*n*)	392	(0; 1453)	2840	(1107; 4593)	0.003
Circumference (µm)	55	(0; 89)	62	(55; 66)	0.58
Σ circumference (mm)	31	(0; 92)	229	(92; 337)	< 0.001
Area (µm^2)	156	(0; 326)	167	(148; 205)	0.83
Σ area (mm^2)	0.12	(0; 0.25)	0.87	(0.35; 1.59)	0.003

strand of roughly equal electron density (Fig. 3b). EDX of several of these needle-like structures revealed calcium and phosphorus peaks exclusively (not shown); on the basis of the calcium k_α peak, the calcium/phosphorus ratio varied between 1.47 and 1.68, consistent with almost mature hydroxyapatite (calcium/phosphorus ratio 1.65). Additional mapping of the elements present in a fixed quadrant of tubular cells from CH-F kidneys vis-à-vis those in the respective quadrant of control kidneys revealed an approximately 5-fold increase of calcium and phosphorus, but surprisingly also of magnesium in the former. As shown previously [46], the three elements were homogeneously distributed within the cells, i.e. they were not confined in a defined compartment, such as the mitochondria. These observations, together with the only mean higher total tissue calcium of the calcified renal medulla (Fig. 2), render uncertain the exact location of precipitating calcium and phosphorus, whether inside or outside cells, or within tubular lumen (also see below).

Lipid deposition and immunohistochemistry

Owing to the impermeability of the calcified matrices, neither cholesterol nor neutral lipids were detected in the calcified areas of the non-decalcified kidney slices; in addition, even after prior decalcification, the reaction for cholesterol was negative. Consequently, it was not possible to determine whether calcium, magnesium, or phosphorus were co-located with, or bound to, intra- or extracellularly deposited lipids. However, in decalcified slices, a positive staining for neutral lipids was present in those areas identified as being calcified, although the specificity of the reaction was low (Fig. 3c). On the other hand, immunohistochemically reacted

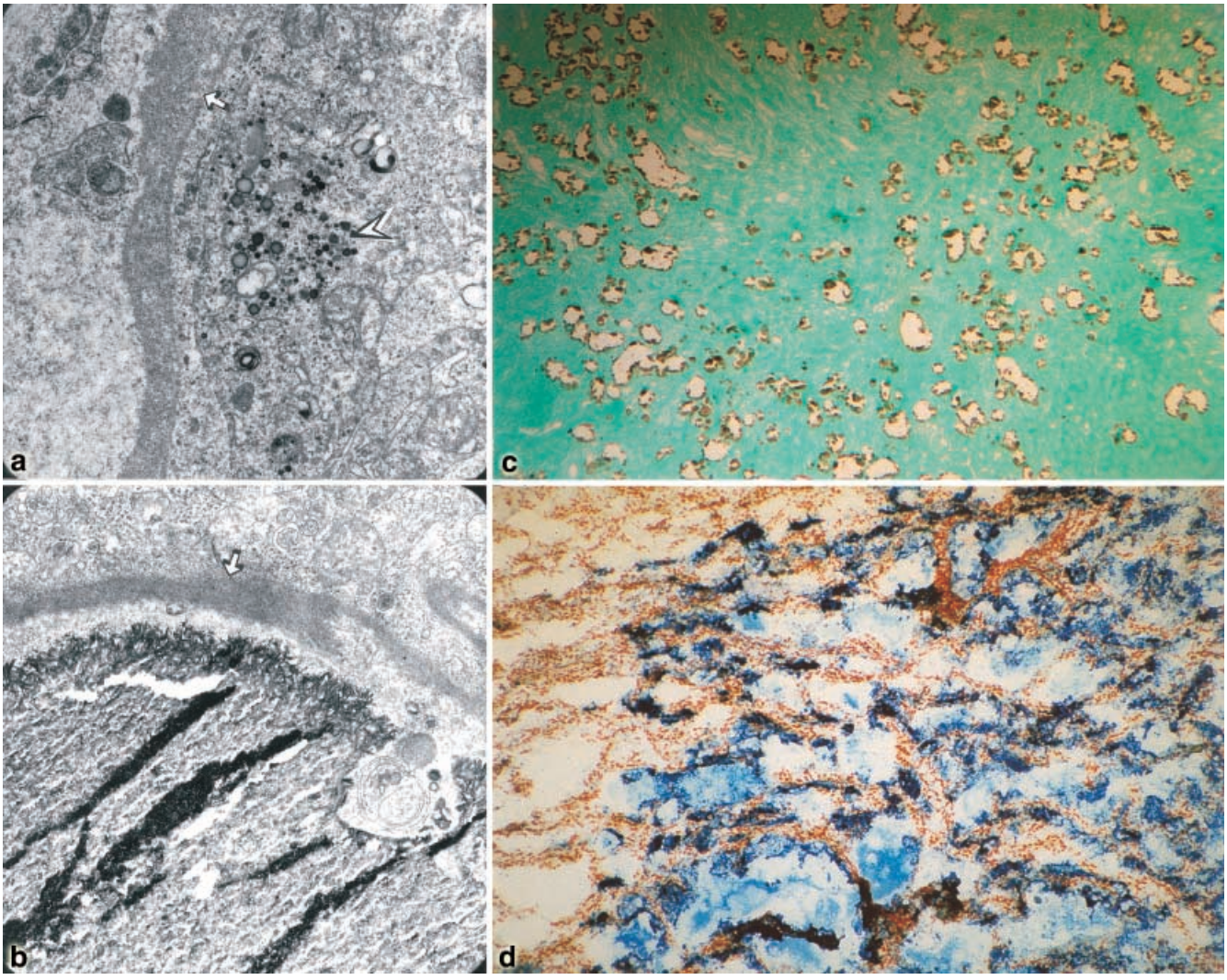

Fig. 3a–d Microscopy of kidney from CH-F rats. **a** Transmission electron microscopy (TEM) of a tubular wall showing a thickened basal membrane of an epithelial cell, containing a number of roundish electron-dense bodies, probably corresponding to lipid droplets (×16,700). **b** TEM of a calcified concretion present in the lumen of a tubule: needle-like crystals are seen at the peripheral border, which appear to be somewhat more electron-dense than the central zone, resembling the situation usually seen in normal and ectopic calcification nodules (×16,700). **c** Light microscopy of the sections stained in accordance to Gallyas and Wolff [19]. Note the brownish calcifications, irregularly distributed in the cortico-medullary region (×100). **d** A segment of the area shown in C following immunochemical tissue treatment with the antibody MC22-33F, detecting choline-containing phospholipids. Note the blue cloudy areas of previously calcified tissue, and the slightly blue reaction in previously unaffected regions (×100)

phospholipids revealed a slightly positive picture in nondecalcified concretions (not shown), but the reaction was clearly positive in the decalcified concretions (Fig. 3d). The latter appeared as roundish or irregular patches, having approximately the same location and distribution as those of the calcified concretions. The staining intensity of the patches was usually uniform, only occasionally being greater along their periphery than in their central zone, suggesting that the phospholipids were homogeneously distributed within them. As expected, the surrounding tissue was also stained. Therefore, and on the basis of the recognition sites of the antibody [8], medullary calcified kidney structures contain phosphatidylcholine, phosphatidylethanolamine, sphingomyelin, or some combination of these, the degree of accumulation of these substances appearing to be dependent on the co-deposited calcium. In the control kidney, the immunoreaction was only slightly positive, and no stained patches were recognizable (not shown).

Minerals in aorta and bone, other variables of bone, markers of bone metabolism, and bone histology

Following random selection from the available aortic wall samples, two from each animal group were pooled to give crude information. Calcium was 11.4 (control) and 8.3 (CH-F) μg/mm vessel length per mg dry tissue; magnesium and phosphorus were undetectably low,

contrasting with abnormally high renal medullary magnesium and phosphorus (Fig. 2), and abnormally low bone calcium (see below).

According to the data in Table 4, CH-F rats had unchanged mean bone density, indicating that there was either no or a parallel shift of underlying bone weight and bone volume (data not shown), and increased ^{45}calcium-specific activity and bone alkaline phosphatase; the decline in exchangeable bone calcium and bone fracturing energy was borderline, but bone calcium was definitely decreased. The bone molar ratio calcium/phosphorus was unchanged (mean values 1.60 and 1.56 for control and CH-F rats, respectively), which is consistent with almost mature hydroxyapatite crystals also found in this organ [21]. Urinary collagen crosslinks – accepted markers of activity of osteoclasts and bone resorption – were only insignificantly higher in CH-F rats than in controls, and osteocalcin – the marker of bone turnover – remained unchanged.

Histologically, there was a tendency toward rarefaction of trabeculae of the more cancellous first lumbar vertebra of CH-F rats, as assessed by trabecular area, and the number, thickness and separation of the trabeculae; several dynamic parameters, including those of bone mineral apposition and bone growth, did not provide better information. Similar data were obtained from the more cortical tibia (data not shown).

Discussion

Because of the virtual absence of information from similarly organized experiments, the following comments focus mainly on the abnormalities observed here.

The NC animal model

Similar to others [28], we also failed to show that an accumulation of calcium and phosphorus in arterial walls is a feature of rats with hypercholesterolemia and hyperlipidemia. The decrease of body weight of NC rats (Fig. 1) – despite comparable food intake (Table 1) – may reflect impaired intestinal absorption of some nutrient(s), and/or energy loss via hyperproteinuria (Table 2). Further dietary crossover studies are needed to clarify whether the abnormal body weight gain is reversible. In contrast, the model appears to be highly suitable for elucidating alterations of minerals in urine, kidney and bone, as well as interactions between minerals and lipids in these two organs. In humans with early signs of renal organ disease, calcium phosphate deposition is frequent and has been intensely studied [20]; often, the former situation is accompanied by dyslipidemia (see below). It follows implicitly that our CH-F rats with dyslipidemic calcium phosphate calcifications may exhibit renal cell disease, the characteristics being increased cellular calcium and phosphorus; such alterations resemble the situation in humans [20]. Compatible with this interpretation is the high phosphorus and calcium content of the renal medulla (Fig. 2), which is the most functionally developed and most vulnerable region.

Additional advantages for renal stone research are seen in the co-incidence of NC, osteopenia, and urinary hyperexcretion of calcium, oxalate and glycolate – a major oxalate precursor – in the presence of unchanged serum minerals and calciotropic hormones, which are frequent findings in calcium stone-forming humans [53]. For example, in patients with idiopathic renal calcium stones, the amount of energy ingested is high due to lipids [50]. Other investigators felt that, for hyperoxaluria and stones to occur in humans, energy intake, the metabolic hormone insulin, and the endogenous pro-

Table 4 Physical data of bone (proximal tibia), bone minerals/unit bone volume, marker substances of bone metabolism in serum (S) and urine (U), and several static parameters from histology of first lumbar vertebra. Values are expressed as the mean, with SE given in parentheses. For technical and other details, see "Materials and methods" and "Results" sections. *SA* specific activity; *Cr* urinary creatinine

	Control $n = 12$		CH-F $n = 12$[a]		*P*-value
Physical data					
Mean density (g/ml)	1.57	(0.006)	1.57	(0.006)	0.34
Fracturing energy (mJ)	163	(21)	124	(9.4)	0.10
^{45}Calcium-SA; [(cpm/μmol) × 10^{-3}]	2.54	(0.07)	2.82	(0.04)	0.002
Exchangeable calcium fraction (%)	13.5	(0.7)	11.8	(0.6)	0.07
Minerals					
Calcium (mmol/ml)	7.95	(0.11)	7.36	(0.16)	0.005
Magnesium (mmol/ml)	0.172	(0.004)	0.163	(0.006)	0.21
Phosphorus (mmol/ml)	4.98	(0.08)	4.73	(0.11)	0.08
Marker substances					
S-osteocalcin (ng/ml)	40	(2)	40	(3)	0.78
S-bone alkaline phosphatase (IU/l)	29	(4)	119	(10)	< 0.001
U-pyridinium/Cr (nmol/mmol)	41	(4)	45	(4)	0.43
U-deoxy-pyridinium/Cr (nmol/mmol)	28	(3)	33	(3)	0.29
Histology					
Tissue area (mm^2)	28.6	(0.47)	27.8	(0.74) [10]	0.19
Trabecular area (mm^2)	0.047	(0.006)	0.041	(0.013 [10]	0.37
Trabecular number (no./mm^2)	1.4	(0.1)	1.3	(0.2) [10]	0.33
Trabecular thickness (μm)	62.7	(2.8)	60.0	(2.1) [10]	0.32
Trabcular separation (μm)	771	(120)	810	(107) [10]	0.41

[a] Except for values in square brackets [ ]

duction of oxalate had to be linked by a simple exponential equation [15]. In fact, under the CH-F diet, i.e. higher intake of energy in the form of lipids, hyperoxaluria did occur. The renal papillary region has long been thought to be the site where calcifications originate [42], but more recent work has identified the medulla [22, 34]. In addition, on the basis of calculations of intratubular solute concentrations in humans, the risk of calcium phosphate precipitation should be highest in the loop of Henle [27, 33], anatomically corresponding with the renal medulla. However, the model may be still suboptimal because calcium phosphate and not calcium oxalate was detected. One explanation for the absence of calcium oxalate crystals could be that, despite the presence of unchanged renal tissue oxalate, oxalate excess may have been restricted to as yet unidentified renal tissue compartments, predisposing them to calcium phosphate NC (also see below).

Hyperlipidemia, and extraosseous and bone minerals

It has long been known that failing renal function has repercussions for circulating lipids, calcium and phosphate, and bone metabolism [43]; the fact that lipid overnutrition, which plagues Western civilizations, can also have repercussions on minerals, bones, and stones has been largely neglected [16, 28]. In the present work, we interpret stable serum calcium to be a consequence of diminished calcium entry into, rather than calcium efflux from, bone (Table 4). Therefore, decreased bone calcium, intrabone calcium redistribution, and some degree of high turnover of bone metabolism have emerged as unwanted sequelae of the CH-F diet. The transient calcium excess in blood should have enabled the CH-F rats to regulate PTH and $1,25(OH)_2D$ at low or normal levels. Defective esterification of calcium-binding phospholipids – substances indispensable for normal mineralization [28] – may have led to anomalous bone. Pointers of incipient bone disease in CH-F rats can be seen in the impaired structure of the truncal and low bone calcium of the appendicular skeleton, the latter accompanied by intrabone calcium redistribution (indicated by ^{45}calcium-specific activity) and increased osteoblast activity (indicated by bone alkaline phosphatase). Calcium that was prevented from entering bone was, at least in part, wasted via urine excretion (Table 2), but the resulting high urinary calcium oxalate and calcium phosphate supersaturation failed to facilitate the formation of stones detectable in the renal pelvis and urinary tract. On the other hand, there is a similarity of processes leading to the deposition of calcium phosphate (hydroxyapatite) in bone and kidney, and these processes include a contribution of anionic proteins, mature collagen, pyrophosphate and adenosine triphosphate (ATP) [1, 2, 7, 28]. The question arises as to whether, in the present work, metabolic alkalosis and hypercitraturia (Table 2) prevented the formation of stones, perhaps in combination with proteinaceous inhibitors of crystallization [9, 40].

Hyperlipidemia and hyperproteinuria

Hyperproteinuria in the presence of LDL- and VLDL-hyperlipoproteinemia is often found in humans with atherosclerosis [24]. The first published investigation on lipid-induced renal tissue damage concluded that glomerular lesions were the first to appear, with those of the tubulo-interstitium appearing later [39]. At the renal interstitial tissue level, lipoproteins can interact with mucoproteins [39], which are substances contributing to the organic matrix of renal stones. In CH-F rats (Table 2), the anatomic site – glomeruli, tubules, or both – in which the hyperexcretion of urinary proteins, especially non-albumin protein(s) originates, is not clear, nor is the true nature of these proteins. If intact glomerular sieves prevented >10-kD blood proteins from reaching the tubular lumen, the urinary proteins of CH-F rats should be products of the tubular epithelium or adjacent tissue. Because these proteins are present together with a tremendous excess of blood LDL- over HDL-bound cholesterol (Table 1), the role of the former may be key to understanding NC in CH-F rats. LDL-bound cholesterol excess is a documented risk factor of atherosclerosis in humans.

Hyperlipidemia, renal minerals and NC

Decades ago, X-ray examination of patients with osteoporosis revealed calcium phosphate calcifications in kidneys, arteries and intervertebral disks [37]. These calcifications were later thought to be due to the actions of phospholipids and a proteinaceous skeleton [2, 17]. Phospholipids are able to impair the sodium/phosphorus co-transport of renal brush border vesicles [68], thereby creating a risk for a deficit of phosphorus relative to calcium at the tissue level (Fig. 2), with deleterious consequences to cell microstructure, viability, and protein shedding into urine. Moreover, in the urine of patients with mixed calcium stones, calcium phosphate crystallization correlates negatively with the non-albumin protein fraction of urine, despite stable physicochemical supersaturation of urine with calcium phosphate [55]. Therefore, on the basis of data in Table 2, the altered spectrum of proteins present in urine (see ''Extracellular minerals and other substances, tissue oxalate and minerals'' subsection), and the phospholipid–calcium interaction (Fig. 3), it may be assumed that the NC in CH-F rats is initiated via hyperlipidemia-mediated alteration of macromolecules rather than of minerals.

Hyperlipidemia, glycolate and oxalate

To date, the combination of hyperlipidemia, NC (with no signs of calcium oxalate co-precipitation in renal

tissue), increased serum LDH, and urinary hyperexcretion of glycolate and oxalate has not been observed. Hyperoxaluria has been observed in rats fed a diet containing 14% fat [38] for 21 days, which is similar to the CH-F diet containing 11% fat. Thus, it cannot be excluded that, in our work, the long-term excess of lipids in the gut lumen complexed intraluminal calcium ions, thereby preventing the intestinal absorption of calcium, but facilitating hyperabsorption of oxalate. However, we used a glycolate-free diet with fixed oxalate content, and this regimen led to a high hepatic oxalate per unit fat-free tissue mass.

Unless disordered hepatic oxalate binding is assumed, the combination of hyperglycoluria and hyperoxaluria should reflect hyperlipidemia-induced increase of oxalate biosynthesis by hepatic peroxisomes. LDH, glycolate oxidase, and glycolate dehydrogenase [4, 69] catalyze the formation of oxalate from glycolate and other oxalate precursors; inhibition of the former two enzymes results in oxalate reduction, while a contribution by the latter is uncertain [69]. LDH, elevated 2-fold in the serum of CH-F rat, is a cytosolic enzyme, while glycolate oxidase and glycolate dehydrogenase are peroxisomal. It is, therefore, reasonable to assume that in the hyperglycoluric and hyperoxaluric CH-F rats the flux of lipids through the cellular metabolic pathways was not properly regulated, and that high plasma LDH, resulting from enzyme overflow to the bloodstream, indicates this situation. In humans, the co-existence of hyperoxaluria and hyperglycoluria has been reported, but is interpreted to be unrelated to primary hyperoxaluria type I [61].

Peroxisomal glycolate oxidation to oxalate is a hydrogen peroxide (H_2O_2) generating process [14, 56]. If not removed by catalase, H_2O_2 leads to oxidative cell damage, in particular impairment of membrane fluidity (synonymous with structural and functional integrity of membranes). The phospholipid phosphatidylethanolamine, which is associated with renal calcifications of CH-F rats (Fig. 3d), is a major constituent of cell membranes, and can be converted to glycolate and oxalate [41]. Thus, a vicious cycle may be initiated by diet-induced hyperlipidemia, ultimately leading to calcifications and cell death. It is unknown whether the latter is initiated by apoptosis (genetically programmed cell death) or necrosis (primary cell swelling followed by destruction of membranes, and extrusion of organelles and cytosol content). The absence of signs of inflammation (see ''Results'' section) seems to indicate apoptosis.

Conclusions

In the light of the data presented, an effect of dietary cholesterol, and probably neutral fat, on the homeostasis of lipids, oxalate, kidney and bone minerals, and the initiation of NC as a possible early event in renal stone formation, for the rat, cannot be ignored. Several of these changes also appear to be amenable to evaluation in renal calcium stone-forming humans, e.g. the lipidemia status, renal oxalate handling, bone mineral density and their relationship to extravascular lipids, and lipid-related parameters associated with pathological calcification of soft tissues. It therefore appears that the performance of appropriate clinical studies would be worthwhile.

Acknowledgements We are grateful to B. Schreiber and K. Schwille for technical assistance, and to I. Goldberg for secretarial work.

References

1. Anderson HC (1969) Vesicles associated with calcification in the matrix of epiphyseal cartilage. J Cell Biol 41: 59
2. Anderson HC (1983) Calcific diseases. A concept. Arch Pathol Lab Med 107: 341
3. Atmani E, Khan SR (1995) Characterization of uronic-acid-rich inhibitor of calcium oxalate crystallization isolated from rat urine. Urol Res 23: 95
4. Bais R, Rofe AM, Conjers RAM (1989) Inhibition of endogenous oxalate production: biochemical considerations of the roles of glycolate oxidase and lactate dehydrogenase. Clin Sci 76: 303
5. Barkin J, Wilson DR, Manuel MA, Bayley A, Murray T, Harrison J (1985) Bone mineral content in idiopathic calcium urolithiasis. Miner Electrol Metab 11: 19
6. Bauer JD (1982) Clinical laboratory methods. CV Mosby, St. Louis
7. Bonucci E (1970) Fine structure and histochemistry of calcifying globules in epiphyseal cartilage. Z Zellforsch Mikrosk Anat 103: 192
8. Bonucci E, Silvestrini G, Mocetti P (1997) MC 22-33F monoclonal antibody shows unmasked polar head groups of choline-containing phospholipids in cartilage and bone. Eur J Histochem 41: 177
9. Boskey AL, Maresa M, Ullrich W, Doty SB, Buthler WT, Prince CW (1993) Osteopontin–hydroxyapatite interaction in vitro: inhibition of hydroxyapatite formation and growth in a gelatin gel. Bone Miner 22: 147
10. Bunce GE, Saacke RG, Mullins J (1980) The morphology and pathogenesis of magnesium deficiency-induced nephrocalcinosis. Exp Mol Pathol 33: 203
11. Carbonneau MA, Peuchant E, Sess D, Canioni P, Clerc M (1991) Free and bound malondialdehyde measured as thiobarbituric acid adduct by HPLC in serum and plasma. Clin Chem 37: 1423
12. Chiang MT, Chen YC, Huang AL (1998) Plasma lipoprotein cholesterol levels in rats fed a diet enriched in cholesterol and cholic acid. Int J Vit Nutr Res 68: 328
13. Cifuentes Delatte L, Minon-Cifuentes JLR, Medina JA (1985) Papillary stones: calcified renal tubules in Randall's plaques. J Urol 133: 490
14. Conyers RAJ, Bais R, Rofe AM (1990) The relation of clinical catastrophes, endogenous oxalate production, and urolithiasis. Clin Chem 36: 1717
15. Conyers RAJ, Fazzalari N, Rofe AM, Bais R (1989) Nutrient energy intake, fasting serum insulin, and urinary oxalate. In: Walker VR, Sutton RAL, Cameron BC, Pak CYC, Robertson WC (eds) Urolithiasis. Plenum Press, New York London, p 643
16. Corrado F, Fini M, Severini G, Roda E (1976) Correlations between renal oxalic lithiasis and cholesterol gall bladder lithiasis. In: Fleisch H, Robertson WG, Smith LH, Vahlensieck W (eds) Urolithiasis research. Plenum Press, New York London, pp 417–422
17. Demer LL (1995) A skeleton in the atherosclerosis closet. Circulation 92: 2029

18. Drach GW, Boyce WH (1972) Nephrocalcinosis as a source for renal stone nuclei. J Urol 107: 897
19. Gallyas F, Wolff JR (1985) Oxalate pretreatment and use of a physical developer render the Kossa method selective and sensitive for calcium. Histochemistry 83: 423
20. Gimenez LF, Solez K, Walker GW (1987) Relation between renal calcium content and renal impairment in 246 human renal biopsies. Kidney Int 31: 93
21. Glimcher MJ (1992) The nature of the mineral component of bone and the mechanism of calcification. In: Coe FL, Favus MJ (eds) Disorders of bone and mineral metabolism. Raven Press, New York, pp 265–286
22. Hering F, Luevend G, Briellmann T, Guggenheim A, Seiler H, Rutishauser G (1985) Calcification sites in humans kidneys – a REM study. In: Schwille PO, Smith LH, Robertson WG, Vahlensieck W (eds) Urolithiasis and related clinical research. Plenum Press, New York, pp 205–208
23. Hess B, Nakagawa Y, Coe FL (1989) Inhibition of calcium oxalate monohydrate crystal aggregation by urine proteins. Am J Physiol 257: F99
24. Kamanna VS, Roh DD, Kirschenbaum MA (1993) Atherogenic lipoproteins: mediators of glomerular injury. Am J Nephrol 13: 1
25. Khan SR, Glenton PA (1996) Increased urinary excretion of lipids by patients with kidney stones. Br J Urol 77: 506
26. Khan SR, Atmani F, Glenton P, Hou ZH, Talham DR, Khurshid M (1996) Lipids and membranes in the organic matrix of urinary calcific crystals and stones. Calcif Tiss Int 59: 357
27. Kok D (1996) Crystallization and stone formation inside the nephron. Scanning Microsc 10: 471
28. Krüger MC, Horrobin DF (1997) Calcium metabolism, osteoporosis and essential fatty acids: a review. Progr Lipid Res 36: 131
29. Lai RK, Goldman P (1992) Urinary organic acid profiles in obese (ob/ob) mice: indications for impaired oxidation of free fatty acids. Metabolism 41: 97
30. Larsson L, Sörbo B, Tiselius HG, Ohman S (1984) A method for quantitative wet-chemical analysis of urinary calculi. Clin Chim Acta 140: 9
31. Lemb B, Geibel K, Kirchhoff S, Lankisch PG (1989) Serum-Carotin: ein einfacher statistischer Laborparameter für die Diagnostik der Steatorrhoe. Dtsch Med Wochenschr 114: 243
32. Lewis PR, Lobban MC (1961) The chemical specificity of the Schultz test for steroids. J Histochem Cytochem 9: 2
33. Luptak I, Bek-Jensen H, Fornander AM, Hojgaard I, Nilsson MA, Tiselius HG (1994) Crystallization of calcium oxalate and calcium phosphate at supersaturation levels corresponding to those in different parts of the nephron. Scanning Microsc 8: 47
34. Malek RS, Boyce WH (1973) Intranephronic calculosis: its significance and relationship to matrix in nephrolithiasis. J Urol 109: 551
35. Manoharan M, Schwille PO (1997) Measurement of oxalate in human plasma ultrafiltrate by ion chromatography. J Chromatogr B 700: 261
36. Marshall RW, Robertson WG (1976) Nomograms for the estimation of the saturation of urine with calcium oxalate, calcium phosphate, magnesium-ammonium phosphate, uric acid, sodium acid urate, ammonium acid urate and cystine. Clin Chim Acta 72: 253
37. Marum GJ (1946) Osteoporosis and calcifications in kidneys, arteries and intervertebral disks. Am J Roentgenol 46: 221
38. Masai M, Ito H (1996) Increased urinary oxalate excretion in rats following a high fat diet. In: Pak CYC, Resnick MI, Preminger GM (eds) Urolithiasis 1996. Millet The Printer, Dallas, pp 177–178
39. Moorhead JF, Chan MK, El-Nahas M, Varghese Z (1982) Lipid nephrotoxicity in chronic progressive glomerular and tubulo-interstitial disease. Lancet 11: 1309
40. Nakagawa Y, Margolis HC, Yokayama S, Kezdy FJ, Kaiser ET, Coe FL (1982) Purification and characterization of a calcium oxalate monohydrate crystal growth inhibitor from human kidney tissue culture medium. J Biol Chem 256: 3936
41. Nath R, Thind SK, Murthy MSR, Talwar HS, Farooqui S (1984) Molecular aspects of idiopathic urolithiasis. In: Baum H, Gergely J, Fanburg BL (eds) Molecular aspects of medicine. Pergamon, Oxford, pp 1–176
42. Randall A (1937) The origin and growth of renal calculi. Ann Surg 105: 1009
43. Ritz E, Heuck CC, Boland R (1979) Phosphate, calcium and lipid metabolism. In: Massry SG, Ritz E, Jahn H (eds) Phosphate and minerals in health and disease. Plenum, London, pp 197–208
44. Rümenapf G, Schwille PO, Erben RG, Schreiber M, Bergé B, Fries W, Schmiedl A, Koroma S, Hohenberger W (1998) Gastric fundectomy in the rat – effects on mineral and bone metabolism, with emphasis on the gastrin–calcitonin–parathyroid hormone–vitamin D axis. Calcif Tiss Int 63: 433
45. Rümenapf G, Schwille PO, Erben RG, Schreiber M, Fries W, Schmiedl A, Hohenberger W (1997) Osteopenia following total gastrectomy in the rat – state of mineral metabolism and bone histomorphometry. Eur Surg Res 29: 209
46. Schmiedl A, Bergé B, Bonucci E, Schwille PO, Grajczyk A (1999) Nephrocalcinosis and hyperoxaluria in the rat fed an atherogenic diet. In: Borghi L, Meschi T, Briganti A, Schianchi T, Novarini A (eds) Kidney stones. Editoriale Bios, Cosenza, pp 461–463
47. Schmiedl A, Schwille PO, Hensen J (1997) Bone mineral density (BMD) in normocalciuric patients with idiopathic calcium urolithiasis (ICU): possible role of urinary calcium, magnesium, phosphate, and magnesium retention from a test meal. In: Jungers P, Daudon M (eds) Renal stone disease. Crystallization process, pathophysiology, metabolic disorders and prevention. Elsevier, Paris, pp 185–187
48. Schmiedl A, Schwille PO, Manoharan M (1996) Lipids in fasting blood, metabolic activity and associated variables in idiopathic calcium urolithiasis of males – a pilot study. In: Pak CYC, Resnick MI, Preminger GM (eds) Urolithiasis. Millet The Printer, Dallas, pp 58–59
49. Schmiedl A, Schwille PO, Bergé B, Markovic M, Dvorak O (1998) Reappraisal of the quantity and nature of renal calcifications, and mineral metabolism in the magnesium-deficient rat – effects of treatment with potassium citrate or the combination magnesium citrate and potassium citrate. Urol Int 61: 76
50. Scholz D, Schwille PO, Sigel A (1981) Ernährungsgewohnheiten von Patienten mit Urolithiasis. Fortschr Urol Nephrol 17: 83
51. Schwille PO, Brandt P, Ulbrich D, Kömpf W (1975) Pankreasinseln, Plasmaglucagon und renale Verkalkungen unter verschiedener Grunddiät bei der Ratte. Urologe A 14: 306
52. Schwille PO, Herrmann U, Schmiedl A, Kissler H, Wipplinger J, Manoharan M (1997) Urinary phosphate excretion in the pathophysiology of idiopathic recurrent calcium urolithiasis: hormonal interactions and lipid metabolism. Urol Res 25: 417
53. Schwille PO, Schmiedl A, Rümenapf G (1998) Management of disorders of calcium metabolism. In: Whitfield HN, Hendry WF, Kirby RS, Duckett JW (eds) Textbook of genitourinary surgery, 2nd edn, vol 1. Blackwell Science, Oxford, pp 771–798
54. Schwille PO, Schmiedl A, Manoharan M, Wipplinger J (1999) Is there a role for uric acid in an animal model of calcium phosphate nephrocalcinosis and calcium phosphate crystallization in urine of patients with idiopathic calcium urolithiasis? An orientational study. J Endourol 13: 637
55. Schwille PO, Schmiedl A, Wipplinger J, Manoharan M (1999) Urinary calcium oxalate and calcium phosphate crystallization in idiopathic calcium urolithiasis. Influence of uric acid. In: Borghi L, Meschi T, Briganti A, Schianchi T, Novarini A (eds) Kidney stones. Editoriale Bios, Cosenza, pp 241–245
56. Selvam GS, Subha K, Varalakshmi P (1992) Effect of L (+)-tartrate on some biochemical and enzymatic parameters in normal and glycolate treated rats. Pharmacol Res 26: 285
57. Sharma V, Schwille PO (1997) Clofibrate feeding to Sprague-Dawley rats increases endogenous biosynthesis of oxalate and causes hyperoxaluria. Metabolism 46: 135

58. Sorensen S, Hansen K, Bak S, Justesen SJ (1990) An unidentified macromolecular inhibitory constituent of calcium oxalate crystal growth in human urine. Urol Res 18: 373
59. Staprans I, Xian-Mang P, Rapp JH, Feingold HHR (1998) Oxidized cholesterol in the diet accelerates the development of aortic atherosclerosis in cholesterol-fed rabbits. Arterioscler Thromb Vasc Biol 18: 977
60. Stout RH, Akin RH, Norton E (1955) Nephrocalcinosis in routine necropsies; its relationship to stone formation. J Urol 74: 8
61. Van Acker KJ, Eyskens FJ, Espeel MF, Wanders RJA, Dekker C, Kerckaert IO, Roels F (1996) Hyperoxaluria with hyperglycoluria not due to alanine:glyoxylate aminotransferase defect: a novel type of primary hyperoxaluria. Kidney Int 50: 1747–1752
62. Varalakshmi G, Radha Shanmuga Sundaram K, Venugopal A (1986) Blood lipids in renal stone disorder. Int J Med Res 66: 840
63. Westlund K (1965) Further observations on the incidence of myocardial infarction in Oslo. J Oslo C Hosp 15: 201
64. Westlund K, Nicolaysen R (1972) Ten-year mortality and morbidity related to serum cholesterol. Scand J Clin Lab Invest (Suppl) 30: 127
65. Westlund K (1973) Urolithiasis and coronary heart disease. A note on association. Am J Epidemiol 97: 167
66. Wojtyczka A, Bergé B, Rümenapf G, Schwille PO, Balanti P, Schreiber M, Fries W, Hohenberger W (1998) Gastrectomy osteopenia in the rat: the role of vitamin B12 deficiency and the type of reconstruction of the digestive tract. Clin Sci 95: 735
67. Yasue T (1969) Histochemical identification of calcium oxalate. Acta Histochem Cytochem 2: 83
68. Zajicek H, Wang H, Kumar V, Wilson P, Levi M (1997) Role of glycosphingolipids in the regulation of renal phosphate transport. Kidney Int (Suppl 61) 52: 3
69. Zakim D, Paradicu RS, Herman RH (1970) Effect of clofibrate (ethylchlorophenoxyisobutyrate) feeding on glycolytic and lipopenic enzymes and hepatic glycogen synthesis in the rat. Biochem Pharmacol 19: 305
70. Zalups RK, Haase P, Philbrick DJ (1983) Phosphate and the development of nephrocalcinosis in rats fed diets containing alpha protein. Am J Pathol 113: 95